Beyond the black-disk limit: from shadow to antishadow scattering mode

S. M. Troshin and N. E. Tyurin
Institute of High Energy Physics, Protvino, Moscow Region, 142284 Russia

Fiz. Élem. Chastits At. Yadra **30**, 1270–1291 (September–October 1999)

A new mode in hadron scattering is predicted to appear at energies beyond $\sqrt{s}\simeq 2$ TeV: the antishadow scattering mode. Experiments on hadronic reactions at LHC and VLHC will be able to reveal it. The appearance of the antishadow scattering mode at these energies is considered on the basis of unitarity and geometrical notions of hadron interactions. Connections with nonperturbative QCD models are discussed. © *1999 American Institute of Physics.* [S1063-7796(99)00405-2]

INTRODUCTION

One of the most fundamental discoveries in hadron interactions at high energies is the rise of the total cross sections with energy. It is accompanied by a rise of the elastic and inelastic cross sections, as well as of the ratio of the elastic to the total cross section.

The total cross-section increase was first observed in K^+p interactions at the Serpukhov accelerator in 1970,[1] and it was discovered later in pp interactions at the CERN ISR[2] and at Fermilab[3] in other nucleon–proton and meson–proton interactions. Recent HERA data[4] demonstrated the rising behavior of the virtual-photon–proton total cross sections. Since then, great progress in experimental and theoretical studies of hadronic reactions has been achieved. Quantum chromodynamics appeared as a theory of strong interactions and gave an explanation for the behavior of the observables in hard hadronic reactions, i.e., reactions with high momentum transfers. However, the dynamics of long-distance interactions (soft processes) is hardly understood despite much work that has been done in this field. This is directly related to the problems of confinement and chiral symmetry breaking.

The approaches to soft hadronic processes are widely varied: Regge-type, geometrical, and QCD-inspired models consider aspects of such processes from different points of view and use various ideas on hadron structure and interaction dynamics. Most of the models consider the global characteristics of hadron interactions, such as $\sigma_{\rm tot}$, $\sigma_{\rm inel}$, and $\sigma_{\rm diff}$, related to large-distance interaction dynamics as reflecting gross features of hadron structure.[5,6] Despite difficulties in applying perturbative QCD for the description of long-distance interactions and their obvious nonperturbative character, it is often possible to represent the high-energy amplitude in various model approaches as an expansion in a small parameter which depends on the kinematics of the process; e.g., for the case of a nonincreasing total cross section the general form of the amplitude is

$$F(s,t)=s\sum_n\,[\tau(s)]^n\exp\left[\frac{a(s)t}{n}\right],$$

where $\tau(s)\sim 1/\ln s$ is a small parameter for $s\to\infty$.

Since the expansion is not valid for rising total cross sections, it is possible to find another representation for that case with a t-dependent expansion parameter:[7]

$$F(s,t)=s\sum_{m=1}^{\infty}\,[\tau(\sqrt{-t})]^m\Phi_m[R(s),\sqrt{-t}],\quad t\neq 0,$$

where

$$\tau(\sqrt{-t})=\exp(-\sqrt{-t}/\mu_0)$$

and $\Phi_m[R(s),\sqrt{-t}]$ is an oscillating function of the momentum transfer. The above formulas as well as some other representations may be successfully used for the phenomenological analysis of the scattering amplitude at high energies.

Thus, the theoretical treatment of soft hadronic reactions now involves a substantial piece of phenomenology and uses various model approaches. They are often based on divergent postulates, but their phenomenological parts are similar. In particular, an amplitude $V(s,t)$ is considered as an input for the subsequent unitarization procedure:

$$F(s,t)=\Phi[V(s,t)].$$

To reproduce the total cross-section rise, the input amplitude $V(s,t)$ is usually considered as a power function of the energy. This function, taken as an amplitude, itself violates unitarity in the direct channel. To satisfy unitarity in the direct channel, a unitarization procedure must be used.

There are several ways to restore unitarity of the scattering matrix. We consider two schemes: those based on the use of the eikonal and the generalized reaction matrix, respectively. There are also combined methods, but those are not often used. As we have already mentioned, various models for $V(s,t)$ may be successfully used to provide a phenomenological description of high-energy hadron scattering. However, in particular model approaches the important dynamical aspects of the interaction could be significantly obscured by a large number of free parameters.

In this paper we discuss some general properties of hadron scattering, the implications of unitarity and analyticity, in particular, manifestations of the antishadow scattering mode, and the respective model predictions for the observables in elastic scattering and diffraction dissociation. Our main goal is to draw attention to the existence of the antishadow

 © 1999 American Institute of Physics

scattering mode at the energies of LHC and VLHC. It might provide new insight into the dynamics of diffraction and head-on hadronic collisions at superhigh energies.

1. GEOMETRICAL PICTURE

In collisions of two high-energy particles the de Broglie wavelength can be short compared with the typical hadronic size, and hence optical concepts may be used as useful guidelines. Thus, hadron scattering can be considered as a collision of two relativistically contracted objects of finite size.

The relevant mathematical tool for the description of high-energy hadronic scattering is based on the impact-parameter representation for the scattering amplitude. In the case of spinless-particle scattering this representation has the following form:

$$F(s,t)=\frac{s}{\pi^2}\int_0^\infty bdbf(s,b)J_0(b\sqrt{-t}). \tag{1}$$

Note that for the scattering of particles with non-zero spin the impact-parameter representation for the helicity amplitudes has a similar form, with the substitution $J_0\to J_{\Delta\lambda}$, where $\Delta\lambda$ is the net helicity change between the final and initial states. As was shown in Ref. 8, the impact-parameter representation is valid for all physical energies and scattering angles. This representation provides a simple semiclassical picture of hadron scattering.

It is often assumed, after the Chou–Yang model was proposed, that the driving mechanism of hadron scattering is due to overlap of the two matter distributions of the colliding hadrons. This could be understood by analogy with the Glauber theory of nuclear interactions: one assumes that the matter density comes from the spatial distribution of the hadron constituents and also assumes a zero-range interaction between those constituents. Such a contact interaction might result from effective QCD, e.g., based on the Nambu–Jona-Lasinio Lagrangian.

An important role in the geometrical approach is played by the notion of the interaction radius. A general definition of the interaction radius which is in agreement with the above geometrical picture was given in Ref. 9:

$$R(s)=l_0(s)/k, \tag{2}$$

where $k=\sqrt{s}/2$ is the particle momentum in the c.m.s. The value of $l_0(s)$ is chosen so that the contributions of the partial-wave amplitudes from angular momenta $l>l_0(s)$ are vanishingly small.

As a first approximation one can consider an energy-independent interaction intensity and describe the elastic scattering amplitude in terms of a black-disk model, where it has the form

$$F(s,t)\propto iR^2(s)\frac{J_1(R(s)\sqrt{-t})}{R(s)\sqrt{-t}} \tag{3}$$

Here $R\sim 1$ fm is the interaction radius. This model is consistent with the observed structure in the differential cross sections of pp and $\bar{p}p$ scattering at t close to 1 $(\mathrm{GeV}/c)^2$.

In the simplest case, neglecting the real part and spin, the impact-parameter amplitude $f(s,b)$ can be obtained as an inverse transformation according to Eq. (1) with

$$F(s,t)\propto\sqrt{s\frac{d\sigma}{dt}(s,t)}.$$

Thus, one can extract information on the geometrical properties of the interaction from the experimental data. The analysis of the experimental data on high-energy diffractive scattering shows that the effective interaction area expands with energy, and the interaction intensity—the opacity—increases with energy at fixed impact parameter b. Such analysis used to be carried out every time new experimental data became available. For example, analysis of the data at the ISR energies (the most precise data set on the differential cross section for a wide t range for $\sqrt{s}=53$ GeV) shows that one can observe a central impact-parameter profile with a tail from the higher partial waves and some suppression (compared to a Gaussian) of low partial waves. The scattering picture at such energies is close to that of a gray disk with a smooth edge which becomes darker at its center with energy.

Besides the above simple geometrical observations, it is useful to keep in mind the rigorous bounds for the experimental observables.

2. BOUNDS FOR OBSERVABLES AND THE EXPERIMENTAL DATA

Bounds for observables obtained on the firm ground of general principles such as unitarity and analyticity are very important for any phenomenological analysis of soft interactions. However, only a few results have been obtained on the basis of axiomatic field theory.

First of all, the Froissart–Martin bound gives an upper limit for the total cross section:

$$\sigma_{\mathrm{tot}}\leqslant C\ln^2 s, \tag{4}$$

where $C=\pi/m_\pi^2$ $(=60\,\mathrm{mb})$ and m_π is the pion mass.

Saturation of this bound, as is suggested by the existing experimental data, implies the dominance of long-distance dynamics. It also leads to a number of important consequences for other observables. For instance, unitarity leads to the following bound for the elastic cross section:

$$\sigma_{\mathrm{el}}(s)\geqslant c\frac{\sigma_{\mathrm{tot}}^2(s)}{\ln^2 s}. \tag{5}$$

Therefore, when the total cross section increases asymptotically as $\ln^2 s$, the elastic cross section must also rise as $\ln^2 s$. It is important to note here that there is no similar bound for the inelastic cross section, and, as we will see later, the absence of such a bound allows for the appearance of the antishadow scattering mode at very high energies.

If one considers a more general case when $\sigma_{\mathrm{tot}}\propto\ln^\gamma s$, then at asymptotic energies one should have

$$\frac{\mathrm{Re}\,F(s,0)}{\mathrm{Im}\,F(s,0)}\simeq\frac{\gamma\pi}{2\ln s} \tag{6}$$

and

$$\frac{\sigma_{\rm tot}^{\bar a}(s)-\sigma_{\rm tot}^{a}(s)}{\sigma_{\rm tot}^{\bar a}(s)+\sigma_{\rm tot}^{a}(s)}\leqslant \ln^{-\gamma/2}(s), \tag{7}$$

where $\sigma_{\rm tot}^{\bar a}(s)$ and $\sigma_{\rm tot}^{a}(s)$ are the total cross sections of the processes $\bar a+b\to X$ and $a+b\to X$, respectively. In the case of $\gamma=2$ the total cross-section difference of the antiparticle and particle interactions should obey the following inequality:

$$\Delta\sigma_{\rm tot}(s)\leqslant \ln s. \tag{8}$$

Unlike the total cross-section behavior, the existing experimental data seem to prefer a decreasing $\Delta\sigma_{\rm tot}(s)$. Possible deviations from such a behavior could be expected on the basis of perturbative QCD,[10] and this was one of the reasons for the recent discussions of the Pomeron counterpart—the odderon. However, recent measurements of the ratio of the real to imaginary part for forward $\bar pp$ scattering provide little support for the odderon. We will not discuss more thoroughly the interesting problem of the $\mathrm{Re}\,F/\mathrm{Im}\,F$ ratio, and we will consider for simplicity the case of a purely imaginary amplitude.

For the slope of the diffraction peak at $t=0$ in the case of a purely imaginary scattering amplitude the following inequality holds:

$$B(s)\geqslant \frac{\sigma_{\rm tot}^2(s)}{18\pi\sigma_{\rm el}(s)}. \tag{9}$$

This means that when the total cross section increases as $\ln^2 s$, the same dependence is mandatory for the slope of the diffraction peak. This is a stronger shrinkage than what the Regge model predicts: $B(s)\sim\alpha'\ln s$.

There is also a bound[11] for the total cross section of single diffractive processes. It was obtained by Pumplin in an approach where both inelastic diffraction and elastic scattering are assumed to arise in the form of a shadow of inelastic processes, and

$$\sigma_{\rm diff}(s,b)\leqslant \frac{1}{2}\sigma_{\rm tot}(s,b)-\sigma_{\rm el}(s,b). \tag{10}$$

The most significant assumption was that the diffractive eigenamplitudes in the Good–Walker[12] picture do not exceed the black-disk limit.

At this point, some details of the experimental situation should be mentioned. At the highest energies, the experimental data on the total and elastic cross sections, the slope parameter of the diffraction peak, and the cross section of single inelastic diffraction dissociation have been obtained in $\bar pp$ collisions at Fermilab. In particular, those measurements show that:

- the rise of the total cross section of $p\bar p$ interactions is consistent with a $\ln^2 s$ dependence, but other dependences are not ruled out;
- the elastic cross section rises faster than the inelastic and total cross sections and is about 1/4 of the total cross section.

Comparing the value of the elastic-to-total cross-section ratio with the lower-energy data, one can conclude that the higher the energy, the higher are both the absolute and the relative probabilities of elastic collisions.

Impact-parameter analysis[13] of the data shows that the scattering amplitude is probably beyond the black-disk limit $|f(s,b)|=1/2$ in head-on collisions. The Pumplin bound [Eq. (10)] is also violated in such collisions, and this is not surprising if we recall the original *ad hoc* assumption about the shadow scattering mode.

3. ANTISHADOW SCATTERING MODE

The basic role in our considerations is played by unitarity of the scattering matrix, $SS^+=1$, which is a reformulation of probability conservation. In the impact-parameter representation the unitarity equation, rewritten for the elastic scattering amplitude $f(s,b)$ at high energies, has the form

$$\mathrm{Im}\,f(s,b)=|f(s,b)|^2+\eta(s,b), \tag{11}$$

where the inelastic overlap function $\eta(s,b)$ is the sum of all inelastic-channel contributions. It can be expressed as a sum of n-particle production cross sections at the given impact parameter:

$$\eta(s,b)=\sum_n \sigma_n(s,b). \tag{12}$$

As has already been mentioned, the assumption of a purely imaginary amplitude is a rather common approximation at high energies and is adequate for our qualitative analysis. Then the unitarity equation (11) shows that the elastic scattering amplitude at a given impact-parameter value is determined by the inelastic processes. Equation (11) implies the constraint

$$|f(s,b)|\leqslant 1,$$

while the black-disk limit presupposes the inequality

$$|f(s,b)|\leqslant 1/2.$$

The equality $|f(s,b)|=1/2$ corresponds to maximal absorption in the partial wave with angular momentum $l\simeq b\sqrt{s}/2$.

The maximal-absorption limit is chosen *a priori* in the eikonal method of unitarization, when the scattering amplitude is written in the form

$$f(s,b)=\frac{i}{2}(1-\exp[i\omega(s,b)]) \tag{13}$$

and an imaginary eikonal $\omega(s,b)=i\Omega(s,b)$ is considered. The function $\Omega(s,b)$ is called the opacity. Eikonal unitarization automatically satisfies the unitarity equation (11) and in the case of a purely imaginary eikonal leads to an amplitude which always obeys the black-disk limit.

However, the unitarity equation has two solutions in the case of a purely imaginary amplitude:

$$f(s,b)=\frac{i}{2}[1\pm\sqrt{1-4\eta(s,b)}]. \tag{14}$$

Eikonal unitarization with a purely imaginary eikonal corresponds to the choice of the particular solution with the minus sign.

Several models have been proposed for the eikonal function. For instance, Regge-type models lead to a Gaussian dependence of $\Omega(s,b)$ on the impact parameter. To provide rising total cross sections the opacity must have a power dependence on the energy:

$$\Omega(s,b)\propto s^{\Delta}\exp[-b^2/a(s)], \tag{15}$$

where $a(s)\sim\ln s$. In the framework of perturbative QCD-based models, the driving contribution to the opacity is due to jet production in gluon–gluon interactions, when

$$\Omega(s,b)\propto\sigma_{\rm jet}\exp[-\mu b], \tag{16}$$

where $\sigma_{\rm jet}\sim(s/s_0)^{\Delta}$. Such parametrizations lead to rising total and elastic cross sections and slope parameters,

$$\sigma_{\rm tot}(s)\sim\sigma_{\rm el}(s)\sim B(s)\sim\ln^2 s, \tag{17}$$

and to the ratio

$$\frac{\sigma_{\rm el}(s)}{\sigma_{\rm tot}(s)}\to\frac{1}{2}. \tag{18}$$

To include the mode in which the scattering amplitude exceeds the black-disk limit, we must consider eikonal functions with nonzero real parts. To ensure the transition from the shadow to the antishadow mode, the real part of the eikonal must gain an abrupt increase equal to π at some $s=s_0$. Conventional models do not foresee such a critical behavior for the real part of the eikonal.

However, this does not mean that the eikonal model itself is in trouble. In particular, allowance for fluctuations of the eikonal[14] strongly modifies the structure of the amplitude and reduces it to an algebraic form similar to that used in the unitarization scheme based on the generalized reaction matrix.

The latter method is based on the relativistic generalization of the Heitler equation of radiation dumping.[15] In this approach the elastic scattering amplitude satisfies the unitarity equation, since it is constructed as a solution of the equation[15]

$$F=U+iUDF, \tag{19}$$

presented here in operator form. Equation (19) allows one to satisfy unitarity, provided that the inequality

$$\operatorname{Im}U(s,b)\geqslant 0 \tag{20}$$

is satisfied. The form of the amplitude in the impact-parameter representation is the following:

$$f(s,b)=\frac{U(s,b)}{1-iU(s,b)}, \tag{21}$$

where $U(s,b)$ is the generalized reaction matrix, which is considered as an input dynamical quantity similar to the eikonal function. A similar form for the scattering amplitude was obtained by Feynman in his parton model of diffractive scattering.[16] The inelastic overlap function is related to $U(s,b)$ by the equation

$$\eta(s,b)=\frac{\operatorname{Im}U(s,b)}{|1-iU(s,b)|^2}. \tag{22}$$

The construction of particular models in the framework of the U-matrix approach proceeds with the same steps as it does for the eikonal function, i.e., the basic dynamics as well as the concepts of hadron structure are used to obtain a particular form for the U matrix. For example, the Regge-pole approach[17] provides the following form for the U matrix:

$$U(s,b)\propto is^{\Delta}\exp[-b^2/a(s)],\quad a(s)\sim\alpha'\ln s, \tag{23}$$

while the chiral quark model, which will be discussed below, gives the exponential b dependence

$$U(s,b)\propto is^{\Delta}\exp[-\mu b], \tag{24}$$

where μ is a constant proportional to the masses of the constituent quarks. We have mentioned here only the gross features of these model parametrizations without going into the details.

Both parametrizations lead to the $\ln^2 s$ rise of the total and elastic cross sections and slope parameter $B(s)$:

$$\sigma_{\rm tot}(s)\sim\sigma_{\rm el}(s)\sim B(s)\sim\ln^2 s \tag{25}$$

for $s\to\infty$. The above results are similar to the conclusions of eikonal unitarization.

However, these two unitarization schemes lead to different predictions for the inelastic cross sections and for the elastic-to-total cross-section ratio. This ratio in the U-matrix unitarization scheme reaches its maximal possible value for $s\to\infty$, i.e.,

$$\frac{\sigma_{\rm el}(s)}{\sigma_{\rm tot}(s)}\to 1, \tag{26}$$

which reflects the fact that the bound for the partial-wave amplitude in the U-matrix approach is $|f|\leqslant 1$, while the bound for the case of an imaginary eikonal is (black-disk limit) $|f|\leqslant 1/2$.

When the amplitude exceeds the black-disk limit (in central collisions at high energies), the scattering at such impact parameters turns out to have an antishadow nature. It corresponds to the solution of the unitarity equation (11) with the plus sign. In this antishadow scattering mode, the elastic amplitude increases with decrease of the inelastic-channels contribution.

The shadow scattering mode is usually considered as the only possible one. But the two solutions of the unitarity equation are equally meaningful, and the antishadow scattering mode could also appear in central collisions first as the energy becomes higher. Both scattering modes are realized in a natural way in the U-matrix approach, despite the fact that the two modes are described by the two different solutions of the unitarity equation (14).

Let us consider the transition to the antishadow scattering mode.[18] With conventional parametrizations of the U matrix in the form (23) or (24) the inelastic overlap function increases with energy at modest values of s. It reaches its maximum value $\eta(s,b=0)=1/4$ at some energy $s=s_0$, and beyond this energy the antishadow scattering mode appears at small values of b. The region of energies and impact

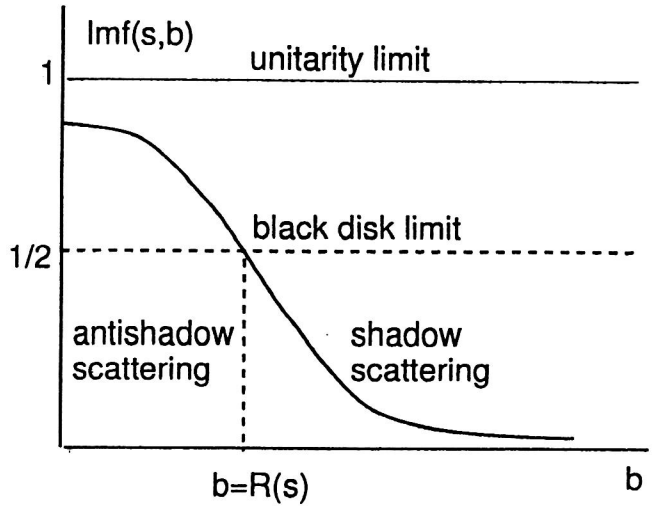

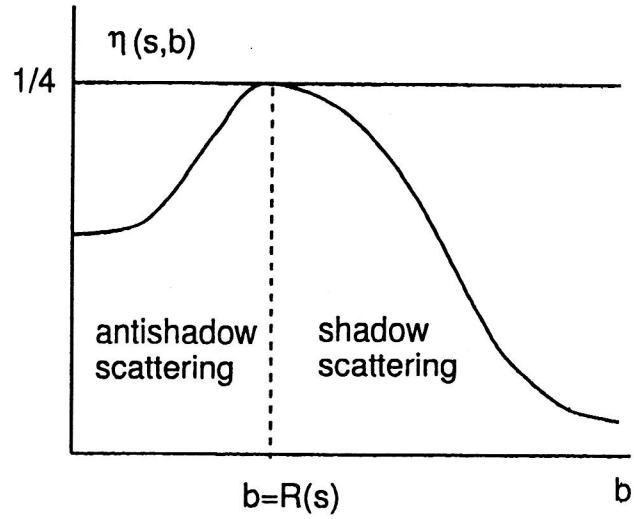

FIG. 1. Shadow and antishadow scattering regions.

parameters corresponding to the antishadow scattering mode is determined by the conditions $\mathrm{Im} f(s,b)>1/2$ and $\eta(s,b)<1/4$. Quantitative analysis of the experimental data[19] gives the threshold value of the energy: $\sqrt{s_0}\simeq 2$ TeV.

Thus, the function $\eta(s,b)$ becomes peripheral when the energy increases. At such energies the inelastic overlap function reaches its maximum value at $b=R(s)$, where $R(s)$ is the interaction radius. Therefore, beyond the transition threshold there are two regions in impact-parameter space: the central region of antishadow scattering for $b<R(s)$ and the peripheral region of shadow scattering for $b>R(s)$. At $b=R(s)$ the maximal absorption (black ring) occurs (Fig. 1).

The transition to the antishadow scattering at small impact parameters at high energies also results in a relatively slow rise of the inelastic cross section:

$$\sigma_{\mathrm{inel}}(s)=8\pi\int_0^\infty \frac{\mathrm{Im}\, U(s,b)}{|1-iU(s,b)|^2}\sim \ln s \tag{27}$$

for $s\to\infty$.

It should be noted that the appearance of the antishadow scattering mode does not contradict the basic idea that particle production is the driving force for elastic scattering. Indeed, the imaginary part of the generalized reaction matrix is the sum of the inelastic-channel contributions:

$$\mathrm{Im}\, U(s,b)=\sum_n \bar{U}_n(s,b), \tag{28}$$

where n runs over all inelastic states and

$$\bar{U}_n(s,b)=\int d\Gamma_n |U_n(s,b,\{\xi_n\})|^2, \tag{29}$$

in which $d\Gamma_n$ is the n-particle element of the phase-space volume. The functions $U_n(s,b,\{\xi_n\})$ are determined by the dynamics of $2\to n$ processes. Thus, the quantity $\mathrm{Im}\, U(s,b)$ itself is a shadow of the inelastic processes. However, unitarity leads to self-damping of the inelastic channels,[20] and increase of the function $\mathrm{Im}\, U(s,b)$ results in decrease of the inelastic overlap function $\eta(s,b)$ when $\mathrm{Im}\, U(s,b)$ exceeds unity.

At the energies when the antishadow mode starts to develop (it presumably could already occur at the energies of the Tevatron Collider) the Pumplin bound (10) for inelastic diffraction dissociation cannot be applied, since the main assumption used in its derivation is no longer valid.

4. THE TWO MODES OF HADRON SCATTERING AND THE PREASYMPTOTIC EFFECTS

In this section we give a specific analysis of hadron scattering on the basis of a particular model. In Refs. 21 and 22 the concepts of the effective chiral quark model were used for the description of elastic scattering at small and large angles. Hadron dynamics was considered in the framework of an effective-Lagrangian approach.

A common feature of chiral models[23] is the representation of a baryon as an inner core carrying the baryonic charge and an outer condensate surrounding this core.[24] Following these observations, it is natural to represent a hadron as consisting of an inner region where the valence quarks are located and an outer region filled with a quark condensate.[22] Such a picture for the hadron structure implies that the overlap and interaction of the peripheral condensates in a hadron collision occurs in the first stage. In the overlap region the condensates interact and, as a result, virtual massive quarks appear. Being released, part of the hadron energy carried by the peripheral condensates goes into generation of massive quarks. Besides mass, the quarks acquire an internal structure and a finite size. The quark radii are determined by the radii of the clouds. The strong-interaction radius of a quark Q is determined by its Compton wavelength:

$$r_Q=\xi/m_Q, \tag{30}$$

where the constant ξ is universal for different flavors. In the model, valence quarks located in the central part of a hadron are assumed to scatter in a quasi-independent way by the produced virtual massive quarks at given impact parameter and by the other valence quarks.

The function $U(s,b)$ (generalized reaction matrix)[15]—the basic dynamical quantity of this approach—is chosen as a product of the averaged quark amplitudes,

$$U(s,b)=\prod_{Q=1}^{N}\langle f_Q(s,b)\rangle, \tag{31}$$

in accordance with the assumed quasi-independent nature of valence-quark scattering. The b dependence of the function $\langle f_Q\rangle$ related to the quark form factor $F_Q(q)$ has the simple form $\langle f_Q\rangle\propto\exp(-m_Qb/\xi)$.

Thus, the generalized reaction matrix (in the purely imaginary case) takes the form

$$U(s,b)=ig\left[1+\alpha\frac{\sqrt{s}}{m_Q}\right]^N\exp(-Mb/\xi), \tag{32}$$

where $M=\Sigma_{q=1}^{N}m_Q$.

At moderate energies $s\ll s_0$ (where $\sqrt{s_0}\equiv m_Q/\alpha$) the function $U(s,b)$ can be represented in the form

$$U(s,b)=ig\left[1+N\alpha\frac{\sqrt{s}}{m_Q}\right]\exp(-Mb/\xi). \tag{33}$$

At very high energies $s\gg s_0$ we can neglect the energy-independent term in (32) and rewrite the expression for $U(s,b)$ as

$$U(s,b)=ig(s/m_Q^2)^{N/2}\exp(-Mb/\xi). \tag{34}$$

The calculation of the scattering amplitude is based on the impact-parameter representation and on the analysis of the singularities of $F(s,\beta)$ in the complex β plane.[7]

Besides the energy dependence of these observables, we emphasize their dependence on the geometrical characteristics of nonperturbative quark interactions.

The total cross section has the following energy and quark-mass dependences:

$$\sigma_{\text{tot}}(s)=\frac{\pi\xi^2}{\langle m_Q\rangle^2}\Phi(s,N), \tag{35}$$

where $\langle m_Q\rangle=(1/N)\Sigma_{Q=1}^{N}m_Q$ is the mean value of the constituent-quark masses in the colliding hadrons. The function Φ has the following behavior:

$$\Phi(s,N)=\begin{cases}(8g/N^2)[1+N\alpha\sqrt{s}/m_Q], & s\ll s_0,\\ \ln^2 s, & s\gg s_0.\end{cases} \tag{36}$$

Thus, at asymptotically high energies the model gives

$$\lim_{s\to\infty}\frac{\sigma_{\text{tot}}(\bar{a}b)}{\sigma_{\text{tot}}(ab)}=1.$$

The (linear with $\sqrt{s}$) preasymptotic rise of the total cross sections is in agreement with the experimental data up to $\sqrt{s}\sim 0.5$ TeV (Ref. 19).

The inelastic cross section can be calculated in the model explicitely, viz.,

$$\sigma_{\text{inel}}(s)=\frac{8\pi\xi^2}{N^2\langle m_Q\rangle^2}\ln\left[1+g\left(1+\frac{\alpha\sqrt{s}}{m_Q}\right)^N\right]. \tag{37}$$

At asymptotically high energies the inelastic cross-section rise is as follows:

$$\sigma_{\text{inel}}(s)=\frac{4\pi\xi^2}{N\langle m_Q\rangle^2}\ln s. \tag{38}$$

For $s\gg s_0$ the dependences of the hadron interaction radius $R(s)$ and the ratio $\sigma_{\text{el}}/\sigma_{\text{tot}}$ on $\langle m_Q\rangle$ are given by the following equations:

$$R(s)=\frac{\xi}{2\langle m_Q\rangle}\ln s, \tag{39}$$

$$\frac{\sigma_{\text{el}}(s)}{\sigma_{\text{tot}}(s)}=1-\frac{4}{N\ln s}. \tag{40}$$

It is important to note here that such a behavior of the ratio $\sigma_{\text{el}}/\sigma_{\text{tot}}$ and $\sigma_{\text{inel}}(s)$ results from self-damping of inelastic channels[20] at small impact distances. Numerical estimates[19] show that the ratio $\sigma_{\text{el}}(s)/\sigma_{\text{tot}}(s)$ becomes close to the asymptotic value 1 at extremely high energies $\sqrt{s}=500$ TeV.

Thus, unitarization drastically changes the scattering picture: at lower energies the inelastic channels provide the dominant contribution and the scattering amplitude has a shadow origin, while at high energies the elastic scattering dominates over the inelastic contribution and the scattering picture corresponds to the antishadow mode. The functional s dependences of the observables also differ significantly. For example, the s dependence of the total cross section for $s\ll s_0$ is described by a simple linear function of $\sqrt{s}$. It has been shown that such a dependence does not contradict the experimental data for hadron total cross sections up to $\sqrt{s}\sim 0.5$ TeV. Such a dependence corresponds to that of a hard Pomeron with $\Delta=0.5$; however, it was obtained in a different approach.[22] This is a preasymptotic dependence, and it has nothing to do with the true asymptotics of the total cross sections. In the model, such behavior of the hadronic cross sections reflects the energy dependence of the number of virtual quarks generated under condensate collisions in the intermediate transient stage of the hadronic interaction.

5. ANTISHADOW SCATTERING MODE AND INELASTIC DIFFRACTIVE PROCESSES

Inelastic diffractive production and elastic scattering at low momentum transfers are the two basic processes which could lead to an understanding of large-distance dynamics and hadron structure. In the case of inelastic diffractive processes this statement can be traced back to the seminal paper of Ref. 12, where such processes were considered as a result of a difference in the absorption of various proton states. Later on, these states acquired a parton-like interpretation. New data were obtained for single diffraction production process

$$h_1+h_2\to h_1+h_2^* \tag{41}$$

when the hadron h_2 is excited to the state h_2^* with invariant mass M and the same quantum numbers. Its subsequent decay results in the multiparticle final state. The inclusive differential cross section shows a simple dependence on the invariant mass:

$$\frac{d\sigma_{\rm diff}}{dM^2}\propto\frac{1}{M^2}. \tag{42}$$

However, the energy dependence of the diffractive-production cross section $\sigma_{\rm diff}(s)$ is not so evident from the data. This ambiguity is partly due to difficulties in the experimental definition of the inelastic diffractive cross section.

The particular experimental regularities observed in diffractive production can be described in the framework of different approaches. The $1/M^2$ dependence is naturally described by the triple-Pomeron diagrams in the framework of the Regge model. The similarity between the Pomeron and photon exchanges proposed in Ref. 25 made it possible to calculate diffractive-dissociation cross sections in terms of the structure function νW_2 measured in deep inelastic lepton scattering. Several models use an optical picture for the description of diffractive production,[26] but these models to a large extent concern the angular distribution of the diffractive cross section, and the M^2 dependence is beyond their scope. An attempt to explain the M^2 dependence in the framework of the optical model by considering diffractive dissociation as bremsstrahlung in which virtual quanta are released from a strong field was made in Ref. 27.

In this section, for the description of single diffractive processes, we use the model approach described in Sec. 4.

To obtain the cross section of the diffractive-dissociation process we must single out among the final states in Eq. (28) those corresponding to the process (41). For simplicity, we consider again the case of a purely imaginary U matrix. Then we can represent $d\sigma_{\rm diff}/dM^2$ in the form

$$\frac{d\sigma_{\rm diff}}{dM^2}=8\pi\int_0^\infty bdb\frac{U_{\rm diff}(s,b,M)}{[1+U(s,b)]^2}, \tag{43}$$

where the expression for $U_{\rm diff}(s,b,M)$ includes contributions from all the final states $|n\rangle_{\rm diff}$ which result from the decay of the excited hadron h_2^* of mass M: $h_2^*\to|n\rangle_{\rm diff}$.

For consideration of the diffractive production at the quark level, we extend the picture for hadron interaction for elastic scattering, as described in Sec. 4. Since a constituent quark is an extended object, there is a nonzero probability of its excitation in the first stage of the hadron collision during the interaction of the peripheral condensates. Therefore it is natural to assume that the origin of the diffractive-production process is the excitation of one of the valence quarks in the colliding hadron, $Q\to Q^*$, and its subsequent scattering and decay into the final state. The excited constituent quark is scattered like other valence quarks in a quasi-independent way. The function $U_{\rm diff}(s,b,M)$ can then be represented as a product

$$U_{\rm diff}(s,b,M)=\langle f_{Q^*}(s,b,M_{Q^*})\rangle\prod_{Q=1}^{N-1}\langle f_Q(s,b)\rangle, \tag{44}$$

where M_{Q^*} is the mass of the excited constituent quark, which is proportional to the mass M of the excited hadron h_2^* for large values of M. This last statement presupposes the additivity of constituent-quark masses. The b dependence of the amplitude $\langle f_{Q^*}\rangle$ is related to the form factor of the excited quark, whose radius is determined by its mass M_{Q^*} ($r_{Q^*}=\xi/M_{Q^*}$). The expression for $U_{\rm diff}(s,b,M)$ can then be rewritten in the form

$$U_{\rm diff}(s,b,M)=g^*U(s,b)\exp[-(M_{Q^*}-m_Q)b/\xi], \tag{45}$$

where the constant g^* is proportional to the relative probability of excitation of the constituent quark. The value of g^* is nonzero, but $g^*<1$, since we expect that the excitation of any constituent quark has lower probability than the probability for this quark to stay unexcited. The excited quark is not stable, and its subsequent decay is associated with the decay of the excited hadron h_2^* into the multiparticle final state $|n\rangle_{\rm diff}$.

The cross section of the diffractive-dissociation process is given by the expression (43) and has the following s and M^2 dependences:

$$\frac{d\sigma_{\rm diff}}{dM^2}\simeq\frac{8\pi g^*\xi^2}{(M_{Q^*}-m_Q^2)^2}\eta(s,0)\simeq\frac{8\pi g^*\xi^2}{M^2}\eta(s,0). \tag{46}$$

Thus, we have obtained the familiar $1/M^2$ dependence of the diffraction cross section, which is related in this model to the geometrical size of the excited constituent quark.

The double-dissociation processes

$$h_1+h_2\to h_1^*+h_2^* \tag{47}$$

can be considered on the basis of the previous approach to single diffractive dissociation. Here one of the constituent quarks in each of the colliding hadrons should be excited. The cross section of the double-diffraction process has similar M^2 and s dependences and is suppressed in comparison with the single diffractive cross section by an extra factor $g^*<1$.

The energy dependence of the single diffractive cross section has the form

$$\sigma_{\rm diff}(s)=8\pi g^*\xi^2\eta(s,0)\int_{M_0^2}^{M_1^2}\frac{dM^2}{M^2}$$

$$=8\pi g^*\xi^2\eta(s,0)\ln\frac{s(1-x_1)}{M_0^2}, \tag{48}$$

where x_1 is the lower limit of the relative momentum of hadron h_1 ($x_1\simeq0.8$–0.9), which corresponds to the experimental constraint on the diffractive process. Equation (48) shows that the total cross section of diffractive dissociation has a nontrivial energy dependence, which is determined by the contribution of inelastic channels to the unitarity equation at zero impact parameter. The dependence of $\eta(s,0)$ is determined by Eq. (22), where the expression for $U(s,b)$ is given by Eq. (32). For $s\leqslant s_0$ (s_0 is determined by the equation $|U(s_0,0)|=1$), $\eta(s,0)$ increases with energy. This increase, as can be seen from Eq. (32) and from the experimental data,[28] is rather slow. However, for $s\geqslant s_0$, $\eta(s,0)$ reaches its maximum value $\eta(s,0)=1/4$, and for $s>s_0$ the function $\eta(s,0)$ decreases with energy. For $s\to\infty$ we have

$$\sigma_{\rm diff}(s)\propto\left(\frac{1}{\sqrt{s}}\right)^N\ln s, \tag{49}$$

since $\eta(s,0)\propto(1/\sqrt{s})^N$ in this limit.

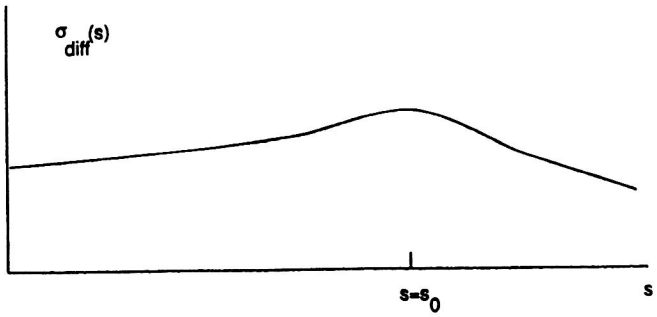

FIG. 2. Energy dependence of the diffractive cross section.

Thus, at asymptotic energies the inelastic diffraction cross section drops to zero. The decrease of the diffractive-production cross section at high energies ($s>s_0$) is due to the fact that $\eta(s,b)$ becomes peripheral for $s>s_0$, and the whole picture corresponds to antishadow scattering for $b<R(s)$ and to shadow scattering for $b>R(s)$, where $R(s)$ is the interaction radius. The qualitative behavior of $\sigma_{\rm diff}(s)$ is shown in Fig. 2.

The development of the antishadow mode in head-on pp and $p\bar{p}$ collisions could be associated with new phenomena in central hadronic collisions, where the temperatures are high and the energy density can be up to several GeV/fm^3. In such collisions the constituent quarks have noticeable probability to be excited. Owing to its high mass and small transverse size, the excited state has low probability of interactions with other particles. It may be also related to an interesting phenomenon in cosmic-ray experiments, where particles with abnormal persistency in lead chambers were observed.[29]

Of course, there might be different reasons for the decrease of $\sigma_{\rm diff}(s)$. A decreasing energy dependence of $\sigma_{\rm diff}(s)$ was also predicted in Refs. 30 and 31. As was pointed out in Ref. 12, in the limit of complete absorption the diffractive dissociation should vanish. It was suggested in Ref. 14 that this situation will occur at superhigh energies and that it is the reason for the decrease of the inelastic diffractive cross section. This is exactly the same behavior as that predicted by our model; however, in our case the reason for this behavior is the transition to the antishadow scattering mode in head-on collisions in the multi-TeV energy range. It should be noted, however, that the diffractive cross section at preasymptotic energies has an energy dependence similar to that of the total and elastic cross sections, and this will be discussed in the concluding part of this paper.

6. UNIVERSAL PREASYMPTOTICS

The straightforward interpretation of the recent HERA data on deep inelastic scattering together with the analysis of data on hadron–hadron scattering in terms of the Regge model could lead to an unexpected conclusion about the existence of various Pomerons[32] or various manifestations of a unique Pomeron in different processes, depending on the typical scale of the process.[33] Approaches[34,35] based on dominance of a soft Pomeron do not rule out the existence of a hard Pomeron.

Indeed, soft hadronic reactions imply that the Pomeron intercept is $\alpha_{\mathcal{P}}=1.08$ (Ref. 32), the small-x dependence of the structure function $F_2(x,Q^2)$ leads to $\alpha_{\mathcal{P}}=1.4-1.5$ (Refs. 36 and 37), and measurements of the diffractive cross section in deep inelastic scattering give $\alpha_{\mathcal{P}}=1.23$ (Ref. 38). So does this mean that we have several Pomerons or that we have several different manifestations of the same Pomeron depending on the particular process? Probably both options should not be considered as firm ones, since the experimental data used to advocate these statements were not obtained at high enough energies where, in fact, the preasymptotic regime of interactions occurs. The above conclusions are based on the presumed dominance of the Pomeron contribution already in the preasymptotic energy region. What is called a Pomeron should be interpreted as a true asymptotic contribution of the driving mechanism.

In this section we argue that all three classes of processes described above are related to similar mechanisms and that the corresponding energy dependences of the cross sections can be well described by a universal energy dependence of the type $a+b\sqrt{s}$. Such a dependence is valid for the preasymptotic energy region only, and beyond this region unitarity changes the picture drastically. We consider for illustration the unitarized chiral quark model (Sec. 4).

Fits to the total hp cross sections give small values for the parameters g and α ($g,\alpha\ll 1$).[19] This means that for $s\ll s_0$ the second term in the square brackets in Eqs. (21) and (22) is small, and we can expand in it. The numerical value of s_0 is determined by the equation $|U(s,0)|=1$ and is[19] $\sqrt{s_0}\simeq 2$ TeV. At this energy the amplitude has the value $|f(s_0,0)|=1/2$. The value of s_0 is on the verge of the preasymptotic energy region, i.e., the Tevatron energy is at the beginning of the road to the asymptotics. Evidently, the HERA energy range $W(=\sqrt{s_{\gamma p}})\leqslant 300$ GeV is in a preasymptotic domain.

The above model gives a dependence linear in $\sqrt{s}$ for the total cross sections according to Eqs. (21) and (22):

$$\sigma_{\rm tot}^{hp,\gamma p}=a+b\sqrt{s}, \tag{50}$$

where the parameters a and b are different for different processes, and the same is true for the scale s_0. It has been shown[19] that Eq. (50) is in good agreement with the experimental data.

The same dependence for the total cross section of γ^*p scattering is assumed by the small-x behavior of the structure function $F_2(x,Q^2)$ (Refs. 36 and 37) and is obtained in Ref. 39:

$$F_2(x,Q^2)=a(Q^2)+b(Q^2)/\sqrt{x}. \tag{51}$$

The experimental data also indicate the critical behavior of the function $b(Q^2)$ at $Q^2\simeq 1$ (GeV/c)^2. This scale could be related to the radius of a constituent quark and its structure.

The third value for the Pomeron intercept $\alpha_{\mathcal{P}}=1.23$ has been obtained from the analysis of experimental data on the diffractive cross section in deep inelastic scattering,[38] where the dependence of $d\sigma^{\rm diff}_{\gamma^*p\to XN}/dM_X^2$ on W was parametrized according to the Regge model and Pomeron dominance was assumed:

$$d\sigma^{\rm diff}_{\gamma^* p\to XN}/dM_X^2 \propto (W^2)^{2\alpha_P - 2}. \quad (52)$$

The data reveal a linear rise of the differential cross section $d\sigma^{\rm diff}_{\gamma^* p\to XN}/dM_X^2$ with W, i.e., we observe here just the same functional dependence on the c.m.s. energy as for $\sigma_{\rm tot}^{hp,\gamma p,\gamma^* p}$. Regarding the preasymptotic nature of the interaction mode, we arrive at the universal c.m.s. energy dependence in the framework of our model.

Indeed, in the framework of this model the hadron inelastic diffractive cross section is given by the expression[40]

$$\frac{d\sigma^{\rm diff}_{hp\to XN}}{dM_X^2} \simeq \frac{8\pi g^* \xi^2}{M_X^2}\,\eta(s,0), \quad (53)$$

where

$$\eta(s,b) = {\rm Im}\, U(s,b)/[1 - iU(s,b)]^2$$

is the inelastic overlap function.

At the preasymptotic energies $s \ll s_0$ the energy dependence of the inelastic diffractive cross section resulting from Eq. (22) is again determined by the generic form

$$\frac{d\sigma^{\rm diff}_{hp\to XN}}{dM_X^2} \propto a + b\sqrt{s}. \quad (54)$$

The inelastic diffractive cross section for $\gamma^* p$ interactions can be obtained by using, for example, the VMD model, i.e.,

$$\frac{d\sigma^{\rm diff}_{\gamma^* p\to XN}}{dM_X^2} \propto a(Q^2) + b(Q^2)W. \quad (55)$$

The same functional dependence can be obtained by using the "aligned-jet" model[41] along with the unitarized chiral quark model.[42]

The above linear dependences for the cross sections of different processes is a generic feature associated with the preasymptotic nature of the interaction dynamics for $s \ll s_0$. As one goes above this energy range, the function $|U(s,b)|$ rises, and when $|U(s,0)| \geqslant 1$ unitarity starts to play the major role and provides the $\ln^2 s$ rise of the total cross sections for $s \gg s_0$ (Ref. 42) and also a behavior of the structure function $F_2(x,Q^2)$ such that

$$F_2(x,Q^2) \propto \ln^2(1/x) \quad (56)$$

for $x \to 0$.[39] At the same time, unitarity leads to a decreasing dependence of the inelastic diffractive cross section for $s \to \infty$,

$$\frac{d\sigma^{\rm diff}}{dM_X^2} \propto \left(\frac{1}{\sqrt{s}}\right)^N, \quad (57)$$

for the hp, γp, and $\gamma^* p$ processes.[40] Equation (57) is associated with the antishadow scattering mode which develops at small impact parameters for $s > s_0$.

Thus, we might expect different asymptotic and universal preasymptotic behaviors for different classes of diffraction processes.

To summarize, we would like to emphasize that a unified description of the processes of hp, γp, and $\gamma^* p$ diffraction scattering with a universal cross-section dependence on the c.m.s. interaction energy is possible. For illustration, we used the unitarized chiral quark model, which has a nonperturbative origin and leads to a linear c.m.s. energy dependence of the cross sections in the preasymptotic energy region for the above processes. Universality of such preasymptotic behavior agrees with experiment.

The assumption about the existence of different Pomerons results from the use of the asymptotic formulas in the preasymptotic energy region and the neglect of unitarity at higher energies beyond this preasymptotic region. It should be taken with some caution.

CONCLUSION

Studies of soft interactions at the highest energies can lead to discoveries of fundamental importance. The genesis of hadron scattering with rising energy can be described as a transition from a gray to a black disk and eventually to a black ring with the antishadow scattering mode at the center. Such transitions are under the control of the unitarity of the scattering matrix.

The appearance of the antishadow scattering mode could be revealed by performing an impact-parameter analysis of elastic scattering and directly in measurements of the inelastic diffractive cross section (cf. Figs. 1 and 2).

It would be interesting to speculate on the particular physical origin of the antishadow scattering mode. Its existence can be correlated with new phenomena expected at high energies in central hadronic collisions. Such collisions are usually associated with the formation of quark–gluon plasma and a disoriented chiral condensate in the inner part of the interaction region. What are the particular correlations between those phenomena and the antishadow scattering? The answer can be obtained in nonperturbative QCD studies and in experiments devoted to studies of soft processes at LHC and VLHC. It seems that the anomalies observed in cosmic-ray experiments[29] might also be correlated with the development of the antishadow scattering mode in central hadron collisions.

[1] S. P. Denisov *et al.*, Phys. Lett. B **36**, 415, 528 (1971).
[2] U. Amaldi *et al.*, Phys. Lett. B **44**, 112 (1973); S. R. Amendolia *et al.*, Phys. Lett. B **44**, 119 (1973).
[3] A. S. Carroll *et al.*, Phys. Lett. B **61**, 303 (1976).
[4] A. Bornheim, Contribution to the LISHEP International School on High-Energy Physics, Rio de Janeiro, Brazil, 1998, hep-ex/9806021.
[5] J. D. Bjorken, Nucl. Phys. B, Proc. Suppl. **25**, 253 (1992).
[6] V. A. Petrov, Talk given at the 5th Blois Workshop on Elastic and Diffractive Scattering, Providence, Rhode Island, 1993.
[7] S. M. Troshin and N. E. Tyurin, Sov. J. Part. Nucl. **15**, 25 (1984).
[8] M. M. Islam, Nucl. Phys. **104**, 511 (1976).
[9] A. A. Logunov, Nguyen Van Hieu, and O. A. Khrustalev, in *Problems of Theoretical Physics* (Nauka, Moscow, 1969).
[10] E. A. Kuraev, L. N. Lipatov, and V. S. Fadin, Sov. Phys. JETP **45**, 199 (1977); Ya. Ya. Balitsky and L. N. Lipatov, Sov. J. Nucl. Phys. **28**, 822 (1978).
[11] J. Pumplin, Phys. Rev. D **8**, 2899 (1973).
[12] M. L. Good and W. D. Walker, Phys. Rev. **120**, 1857 (1960).
[13] S. Belforte, CDF Collaboration, Nuovo Cimento A **107**, 2085 (1994).
[14] S. Barshay, P. Heiliger, and D. Rein, Z. Phys. C **56**, 77 (1992).
[15] A. A. Logunov, V. I. Savrin, N. E. Tyurin, and O. A. Khrustalev, Teor. Mat. Fiz. **6**, 157 (1971).
[16] F. Ravndal, Int. J. Mod. Phys. A **8**, 4369 (1993).
[17] N. E. Tyurin and O. A. Khrustalev, Teor. Mat. Fiz. **24**, 291 (1975).
[18] S. M. Troshin and N. E. Tyurin, Phys. Lett. B **316**, 175 (1993).

[19] P. M. Nadolsky, S. M. Troshin, and N. E. Tyurin, Z. Phys. C **69**, 131 (1995).
[20] M. Baker and R. Blankenbecler, Phys. Rev. **128**, 415 (1962).
[21] S. M. Troshin, N. E. Tyurin, and O. P. Yuschenko, Nuovo Cimento A **91**, 23 (1986).
[22] S. M. Troshin and N. E. Tyurin, Nuovo Cimento A **106**, 327 (1993); *Proceedings of the 5th Blois Workshop on Elastic and Diffractive Scattering*, Providence, Rhode Island, 1993, p. 387; Phys. Rev. D **49**, 4427 (1994); Z. Phys. C **64**, 311 (1994).
[23] R. D. Ball, Int. J. Mod. Phys. A **5**, 4391 (1990).
[24] M. M. Islam, Z. Phys. C **53**, 253 (1992).
[25] A. Donnachie and P. V. Landshoff, Phys. Lett. B **185**, 403 (1987); Nucl. Phys. B **311**, 509 (1988).
[26] R. S. Fletcher, Phys. Rev. D **46**, 187 (1992).
[27] K. H. Dederichs and M. A. Fassler, Phys. Lett. B **232**, 405 (1989).
[28] H. I. Miettinen and J. Pumplin, Phys. Rev. D **18**, 1696 (1978).
[29] M. G. Albrow, Summary talk given at the 5th Blois Workshop on Elastic and Diffractive Scattering, Providence, Rhode Island, 1993.
[30] T. Chou and C. N. Yang, Phys. Rev. D **32**, 1692 (1985).
[31] L. Durand and H. Pi, Phys. Rev. D **38**, 78 (1988).
[32] P. V. Landshoff, Talk given at the PSI School at Zuos, 1994; M. Bertini, M. Giffon, and E. Predazzi, Preprint, INFN, 1995.
[33] A. Levy, Talk given at the International Europhysics Conference on High Energy Physics, Brussels, 1995; M. Bertini, M. Giffon, L. L. Jenkovszky, F. Paccanoni, and E. Predazzi, Riv. Nuovo Cimento **19**, 1 (1996).
[34] A. Donnachie and P. V. Landshoff, J. Phys. G **22**, 733 (1996).
[35] V. A. Petrov, Talk given at the High Energy Conference on Quantum Chromodynamics—QCD '96, Montepellier, France, 1996; Preprint IHEP 96–69.
[36] H1 Collaboration, Nucl. Phys. B **407**, 515 (1993); **439**, 379 (1995).
[37] ZEUS Collaboration, Phys. Lett. B **316**, 412 (1993); Z. Phys. C **65**, 379 (1995).
[38] ZEUS Collaboration, Z. Phys. C **70**, 391 (1996).
[39] S. M. Troshin and N. E. Tyurin, Europhys. Lett. **37**, 239 (1997).
[40] S. M. Troshin and N. E. Tyurin, Z. Phys. C **64**, 311 (1994).
[41] J. D. Bjorken and J. Kogut, Phys. Rev. D **8**, 1341 (1973); S. J. Brodsky, P. Hoyer and L. Magnea, NORDITA-96/68P, SLAC-PUB-7342, hep-ph/9611278.
[42] S. M. Troshin and N. E. Tyurin, Nuovo Cimento A **106**, 327 (1993); in *Proceedings of the 5th Blois Workshop on Elastic and Diffractive Scattering*, Providence, Rhode Island, 1993, edited by H. M. Fried, K. Kang, and C.-I. Tan, p. 387; Phys. Rev. D **49**, 4427 (1994).

This article was published in English in the original Russian journal. It is reproduced here with stylistic changes by the Translation Editor.